THE JOURNAL OF BIOLOGICAL CHEMISTRY VOL. 288, NO. 44, pp. 31528–31539, November 1, 2013

Dragon (Repulsive Guidance Molecule RGMb) Inhibits E-cadherin Expression and Induces Apoptosis in Renal Tubular Epithelial Cells*

Received for publication, September 10, 2013, and in revised form, September 19, 2013 Published, JBC Papers in Press, September 19, 2013,
DOI 10.1074/jbc.M113.517573

Wenjing Liu[‡1], Xiaoling Li[‡], Yueshui Zhao[‡1], Xiao-Ming Meng[§], Chao Wan[‡¶], Baoxue Yang[‖], Hui-Yao Lan[§], Herbert Y. Lin[2], and Yin Xia[‡¶3]**

*From the [‡]Key Laboratory for Regenerative Medicine, Ministry of Education, School of Biomedical Sciences, Faculty of Medicine, The Chinese University of Hong Kong, Hong Kong, China, [¶]School of Biomedical Sciences Core Laboratory, The Chinese University of Hong Kong Shenzhen Research Institute, Shenzhen 518057, China, **Program in Anemia Signaling Research, Division of Nephrology, Program in Membrane Biology, Center for Systems Biology, Department of Medicine, Massachusetts General Hospital, Harvard Medical School, Boston, Massachusetts 02114, [§]Li Ka Shing Institute of Health Sciences and Department of Medicine and Therapeutics, The Chinese University of Hong Kong, Hong Kong, China, and [‖]Department of Pharmacology, School of Basic Medical Sciences, Peking University and Key Laboratory of Molecular Cardiovascular Sciences, Ministry of Education, Beijing 100191, China*

Background: Dragon is expressed in kidney tubular epithelial cells.
Results: Dragon inhibits E-cadherin expression and induces apoptosis in IMCD3 cells, and Dragon$^{+/-}$ mice exhibit increased E-cadherin expression and decreased apoptosis in injured renal tubules.
Conclusion: Dragon inhibits E-cadherin and induces apoptosis in renal tubular cells both *in vitro* and *in vivo*.
Significance: Our results provide a novel mechanism underlying kidney injury.

Dragon is one of the three members of the repulsive guidance molecule (RGM) family, *i.e.* RGMa, RGMb (Dragon), and RGMc (hemojuvelin). We previously identified the RGM members as bone morphogenetic protein (BMP) co-receptors that enhance BMP signaling. Our previous studies found that Dragon is highly expressed in the tubular epithelial cells of mouse kidneys. However, the roles of Dragon in renal epithelial cells are yet to be defined. We now show that overexpression of Dragon increased cell death induced by hypoxia in association with increased cleaved poly(ADP-ribose) polymerase and cleaved caspase-3 levels in mouse inner medullary collecting duct (IMCD3) cells. Dragon also inhibited E-cadherin expression but did not affect epithelial-to-mesenchymal transition induced by TGF-β in IMCD3 cells. Previous studies suggest that the three RGM members can function as ligands for the receptor neogenin. Interestingly, our present study demonstrates that the Dragon actions on apoptosis and E-cadherin expression in IMCD3 cells were mediated by the neogenin receptor but not through the BMP pathway. Dragon expression in the kidney was up-regulated by unilateral ureteral obstruction in mice. Compared with wild-type mice, heterozygous Dragon knock-out mice exhibited 45–66% reduction in Dragon mRNA expression, decreased epithelial apoptosis, and increased tubular E-cadherin expression and had attenuated tubular injury after unilateral ureteral obstruction. Our results suggest that Dragon may impair tubular epithelial integrity and induce epithelial apoptosis both *in vitro* and *in vivo*.

Dragon (RGMb) is one of the three repulsive guidance molecule (RGM)[4] family members RGMa, RGMb (Dragon), and RGMc (hemojuvelin). RGM family members are glycophosphatidylinositol-anchored membrane proteins. We identified the three RGM proteins as co-receptors that enhance BMP-Smad signaling (1–5). Our previous studies showed that the Dragon protein is expressed in the epithelial cells of kidney tubules including collecting ducts, distal convoluted tubules, and thick ascending limbs and that Dragon enhances BMP4 signaling in tubular epithelial cells (6). These data suggest that Dragon may play a role in kidney epithelial function.

BMPs are members of the TGF-β superfamily of multifunctional ligands. It is well documented that BMPs play an important role in nephrogenesis (7), but the role of BMPs in the adult kidney is less well understood. Our previous study demonstrated that BMPs, including BMP-2, -4, -5, -6, and -7, are expressed in the adult mouse kidney (6). Furthermore, BMP

* This work was supported by the Hong Kong Research Grant Council (RGC) and National Natural Science Foundation of China (NSFC) joint grants N_CUHK432/12 and 81261160507 (to Y. X. and B. Y.), the startup fund offered by The Chinese University of Hong Kong (to Y. X.), RGC/General Research Fund (GRF) grant CUHK477311 (to Y. X.), CUHK direct grants 2041603 and 2041747 (to Y. X.), Shenzhen Science and Technology Research and Development Funding SZRI-C.02.12.006 (to Y. X.), and National Institute of Health Grants RO1 DK-069533 and RO1 DK-071837 (to H. Y. L.).
[1] Supported by Chinese University of Hong Kong postgraduate scholarships.
[2] To whom correspondence may be addressed: Program in Membrane Biology, Richard B. Simches Research Center, 185 Cambridge St, CPZN-8216, Boston, MA 02114. Tel.: 617-726-5661; Fax: 617-643-3182; E-mail: Lin.Herbert@mgh.harvard.edu.
[3] To whom correspondence may be addressed: School of Biomedical Sciences, The Chinese University of Hong Kong, Shatin, N.T., Hong Kong, China. Tel.: 852-39434480; Fax: 852-26035123; E-mail: Xia.Yin@cuhk.edu.hk.

[4] The abbreviations used are: RGM, repulsive guidance molecule; BMP, bone morphogenetic proteins; UUO, unilateral ureteric obstruction; EMT, Epithelial-to-mesenchymal transition; α-SMA, α-smooth muscle actin; Het, heterozygous Dragon knock-out; MTT, 3-(4,5-dimethylthiazol-2-yl)-2,5-diphenyltetrazolium bromide.

receptor expression has also been described (8), supporting the notion that the adult kidney can respond to BMP stimulation. A large body of evidence suggests that BMP signaling should exert a protective action on renal tubules in kidney injury (9–13).

Neogenin is a member of the immunoglobulin superfamily of transmembrane receptors. Neogenin is a receptor for RGMa. The RGMa-neogenin interaction plays a role in regulating apoptosis. Neogenin also interacts with Dragon with high affinity, and Dragon inhibits neurite growth and cell migration through neogenin (14). Recently, the crystal structures of the complex of RGMb and neogenin ectodomains were resolved (15). Neogenin is highly expressed in kidney tubular epithelial cells (16), where Dragon is also expressed. Whether the Dragon and neogenin interaction plays a role in renal epithelial cells remains to be investigated.

Kidney injury is a major clinical problem. In response to hemodynamic, hypoxic, mechanical, and chemical insults, tubular epithelial cells undergo morphologic changes, loss of polarity, and cell death. Tubular epithelial cell death is a process that is closely associated with tubular atrophy and tubulointerstitial fibrosis of the kidney (17–20). In the case of unilateral ureteric obstruction (UUO), tubular epithelial cell death occurs principally through apoptosis (21). Tubular epithelial cell apoptosis can be triggered by many factors including mechanical stretching, oxidant stress, and hypoxia. The importance of apoptosis in kidney injury is demonstrated by previous studies showing that inhibition of apoptosis reduced renal injury (19, 22).

Epithelial-to-mesenchymal transition (EMT) is a process characterized by loss of epithelial proteins such as E-cadherin and cytokeratin and gain of mesenchymal markers including vimentin, α-smooth muscle actin (α-SMA), and extracellular matrix components including collagens (23, 24). It is well established that tubular epithelial cells *in vitro* can indeed transform into fibroblasts and myofibroblasts when incubated with TGF-β1 and other fibrogenic insults. An intensive body of evidence purports to show that EMT also occurs *in vivo* in many animal models of chronic kidney diseases and in human kidney biopsies from various progressive kidney diseases (23, 24). However, recent studies using genetic lineage tracing methods failed to show that renal tubular epithelial cells acquire mesenchymal markers *in vivo* in renal fibrosis models (25–27).

Here, we show that Dragon increased hypoxia-induced cell death and inhibited E-cadherin expression in IMCD3 cells. Dragon did not have any effect on TGF-β1-induced EMT in IMCD3 cells. Compared with WT mice, heterozygous Dragon knock-out mice exhibited decreased cell apoptosis and increased E-cadherin expression in tubular epithelial cells and had attenuated tubular injury in obstructed kidneys. Our results have revealed previously unidentified biological roles for Dragon in renal tubular injury.

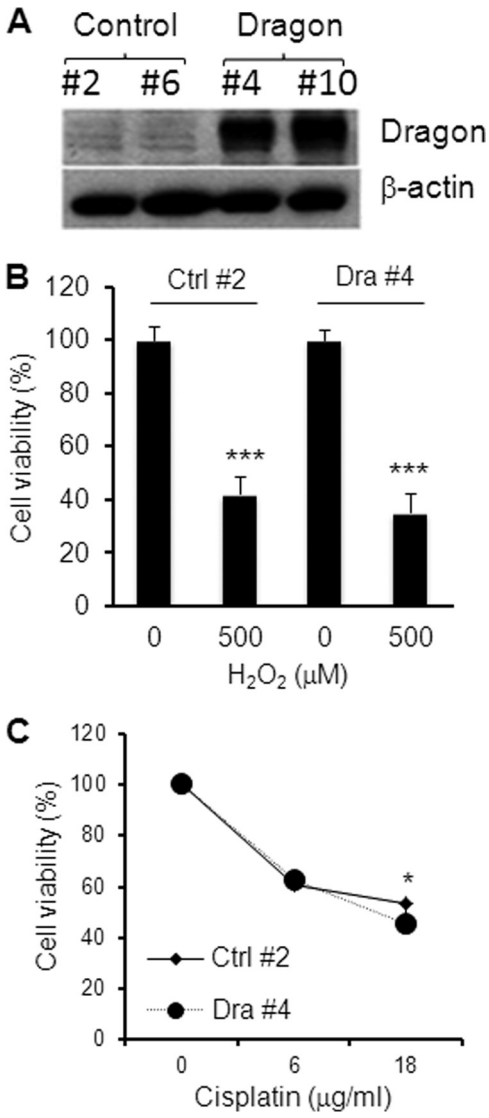

FIGURE 1. **Dragon has no major effect on cell death induced by H_2O_2 and cisplatin in IMCD3 cells.** *A*, Western blotting analysis of Dragon expression in stable cell lines Dra#4 and Dra#10 in comparison with control cell lines Ctrl#2 and Ctrl#6. β-Actin was used as loading control. *B*, control cells (Ctrl#2) or Dragon-overexpressing cells (Dra#4) were incubated with and without H_2O_2 at 500 μM for 48 h before being subjected to MTT assay ($n = 10$). The viability of cells incubated with H_2O_2 was normalized to the viability of cells incubated without H_2O_2. *C*, Ctr#2 and Dra#4 were incubated with increasing doses of cisplatin for 24 h before being subjected to MTT assay ($n = 10$). The viability of cells incubated with cisplatin was normalized to the viability of cells incubated without Cisplatin. *, $p < 0.05$; ***, $p < 0.001$.

EXPERIMENTAL PROCEDURES

Transfection and Selection of Stably Expressing Clones—IMCD3 cells (ATCC CRL-2123) were cultured in DMEM medium (Invitrogen) supplemented with 10% FBS. Cells were transfected with pcDNA3.1 or Dragon expression construct using Lipofectamine 2000 (Invitrogen) according to the manufacturer's instructions. 48 h after transfection, 600 μg/ml G418 and 500 μg/ml Zeocin were added to the cells transfected with pcDNA3.1 and cells transfected with Dragon construct, respectively, and colonies were screened for Dragon protein expression by Western blotting. Two control lines (Ctrl#2, and Ctrl#6) and two Dragon-overexpressing (Dra#4 and Dra#10) lines were used for this study.

MTT Assays—To determine the role of Dragon in cell death induced by hypoxia, control cells and Dragon-overexpressing cells were cultured in 96-well plates for 72 h in a hypoxia atmosphere containing 2% O_2. Cell viability was measured by MTT assay kit (Sigma). Cells cultured under normal conditions were used to normalize the viability of cells cultured under hypoxia.

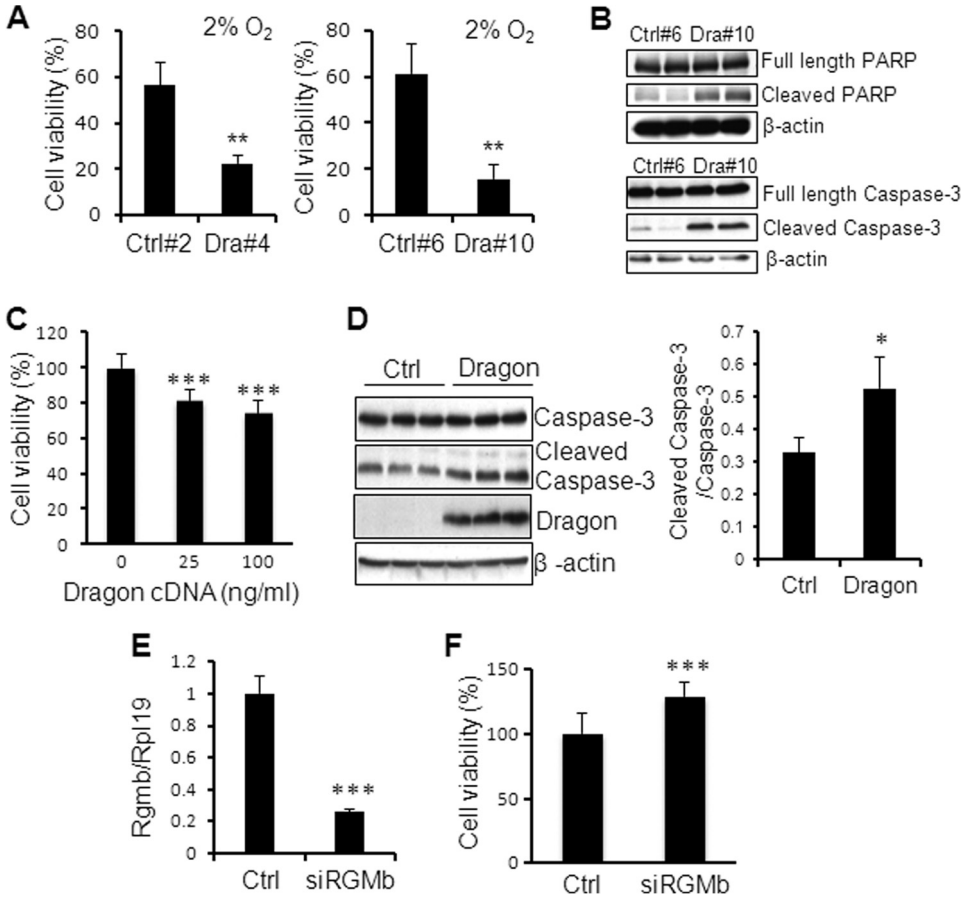

FIGURE 2. **Dragon (RGMb) increases cell death in IMCD3 cells under hypoxia.** *A*, control cells (Ctrl#2 and Ctrl#6) or stable Dragon-overexpressing cells (Dra#4 and Dra#10) were cultured in 2% O_2 or under normal conditions for 72 h before being subjected to MTT assay ($n = 10$). The viability of cells cultured in hypoxia was normalized to the viability of cells cultured under normal conditions. *B*, Ctrl#6 or Dra#10 cells were cultured for 48 h in 2% O_2 before being subjected to Western blotting for poly(ADP-ribose) polymerase (*PARP*), caspase-3, and β-actin. *C*, IMCD3 cells were transiently transfected with increasing amounts of Dragon cDNA. 24 h after transfection cells were cultured in 2% O_2 before being subjected to MTT assay ($n = 10$). *D*, IMCD3 cells were transiently transfected with Dragon cDNA. 24 h after transfection cells were cultured in 2% O_2 before being subjected to Western blotting for caspase-3, Dragon, and β-actin (*left panel*). Densitometric analysis was performed to determine cleaved caspase-3 relative to full-length caspase-3 (*right panel*). *E*, inhibition of RGMb expression by siRGMb. IMCD3 cells were transfected with control (*Ctrl*) or RGMb siRNA (*siRGMb*, 60 nM). 72 h after transfection cells were collected for real time PCR analysis for RGMb mRNA levels. Rpl19 is the internal control ($n = 3$). *F*, effects of inhibition of RGMb expression on cell viability under hypoxia. IMCD3 cells transfected with control or RGMb siRNA were cultured for 72 h in 2% O_2 ($n = 8$) before being subjected to MTT assay. *, $p < 0.05$; **, $p < 0.01$; ***, $p < 0.001$.

Some control cells and Dragon-overexpressing cells were incubated with and without 500 μM H_2O_2 for 48 h before the cells were analyzed for viability. Additional control and Dragon-overexpressing cells were incubated with increasing concentrations of cisplatin (0, 6, 18 μg/ml) for 24 h before MTT assays were performed.

EMT Assays—To determine the time-course of TGF-β1 in epithelial transformation, IMCD3 cells at 30–40% confluence were serum-starved overnight before the cells were incubated with or without 5 ng/ml TGF-β1 in DMEM containing 10% FBS for 0, 1, 2, 4, 8, 24, 48, and 72 h. The cells were then harvested to measure the levels of mRNA for E-cadherin, α-SMA, and vimentin.

To test whether Dragon has any effects on TGF-β1-induced EMT, IMCD3 cells were transiently transfected with and without Dragon. 24 h after transfection, the cells were incubated for 48 h with and without 5 ng/ml TGF-β1 in DMEM containing 10% FBS. The cells were then harvested to measure the levels of Dragon, E-cadherin, and α-SMA.

siRNA Targeting—To test whether inhibition of Dragon and/or neogenin expression affects cell viability or E-cadherin expression, IMCD3 cells were transfected with scrambled control siRNA, a mixture of two Dragon siRNA sequences (siRGMb, 60 nM), a mixture of two neogenin sequences (siNeo1, 60 nM), a combination of Dragon cDNA and siNeo1, or a combination of siRGMb and siNeo1 using Lipofectamine 2000 or DharmaFECT Transfection Reagents (Thermo Scientific). Scrambled control siRNAs were purchased from Ambion. The previously described Dragon siRNA sequences (28) were purchased from Ambion. Mouse neogenin siRNAs were purchased from Shanghai GenePharma Co., Ltd (Shanghai, China). A mixture of the following two neogenin siRNA sequences were used: 5′-CCUGGGAUCUGACUACAAATT-3′; 5′-GGACAUUGUAUUUGAAUGUTT-3′. Approximately 24 h after transfection, some cells were incubated in 2% O_2 for 48–72 h before MTT assays or Western blotting for caspase-3, and other cells were maintained in the complete medium before being subjected to real time PCR and Western blotting to analyze Dragon, neogenin, and E-cadherin expression.

UUO—The generation, characterization, and genotyping of Dragon KO mice (57/B6/129) have been described previously (28). Male WT and Dragon$^{+/-}$ mice at 3–4 months of age were

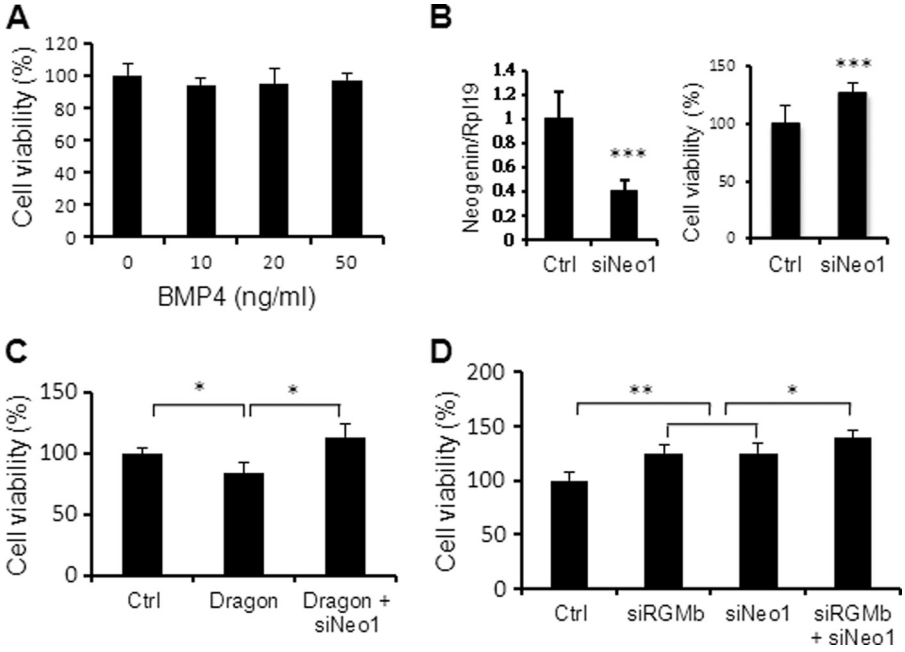

FIGURE 3. **Dragon (RGMb) inhibits cell viability through the neogenin receptor but not the BMP pathway in IMCD3 cells under hypoxia.** *A*, BMP4 does not regulate IMCD3 cell viability. Cells were cultured in 2% O_2 in the presence of increasing amounts of BMP4 (0–50 ng/ml) for 72 h. Cells were then subjected to MTT assay. *B*, inhibition of neogenin expression increases cell viability. IMCD3 cells transfected with control or neogenin siRNA (*siNeo1*, 60 nM) were cultured for 72 h in 2% O_2 before being subjected to MTT assay or real time PCR analysis for neogenin mRNA expression. *C*, inhibition of neogenin expression restored cell viability reduced by Dragon in IMCD3 cells. Cells were transfected with Dragon cDNA or Dragon cDNA in combination of neogenin siRNA (*siNeo1*). Cells were cultured for 72 h in 2% O_2 before being subjected to MTT assay. *D*, double inhibition of Dragon (RGMb) and neogenin further increased cell viability. IMCD3 cells were transfected with RGMb siRNA (*siRGMb*), neogenin siRNA (*siNeo1*) or both. Cells were cultured for 72 h in 2% O_2 before being subjected to MTT assay. *, $p < 0.05$; **, $p < 0.01$; ***, $p < 0.001$. $n = 3$ for real time PCR analysis; $n = 8$ for MTT assays.

subjected to UUO surgery through a left flank incision. The ureter was identified and tied at the level of the lower pole of the kidney with two separate silk ties. The mice were sacrificed 3 or 7 days after the UUO surgeries. All the procedures were performed in accordance with Animal Experimentation Ethics Approval by The Chinese University of Hong Kong Animal Experimentation Ethics Committee.

Histology and Immunofluorescence—Paraffin kidney sections were used for periodic acid-Schiff staining. The degree of tubular damage including tubular dilation, tubular atrophy, and cast formation was scored by three investigators without knowing the genotypes. Masson's Trichrome Staining was used to examine interstitial collagen deposits.

Cryosections were used for immunofluorescent staining to detect macrophage infiltration and E-cadherin. Sections were treated with 1% SDS for 4 min. The sections were incubated with F4/80 antibodies (Abcam) or anti-E-cadherin antibodies (clone DECMA-1, Santa Cruz Biotechnology) followed by Cy3-labeled secondary antibodies. 10 fields per section and three sections per kidney were examined for each animal to determine the F4/80-positive macrophages per field using ImageJ.

TUNEL Assays—Apoptotic cells in paraffin kidney sections were identified using ApopTag Plus Fluorescein *In Situ* Apoptosis Detection kit (Chemicon International) according to the manufacturer's instructions. 10 fields per section and three sections per kidney were examined for each animal to determine the apoptotic tubular epithelial cells per field or the apoptotic tubular epithelial cells over the total number of cells using ImageJ.

Western Blotting—Kidney tissues and IMCD3 cells were lysed as described previously (6). A total of 20–40 μg of protein was separated by SDS-PAGE and transferred to polyvinylidene difluoride membranes. Membranes were probed with anti-E-cadherin (BD Biosciences), anti-α-SMA (Abcam), anti-PARP (poly(ADP-ribose) polymerase) (Cell Signaling Technology), anti-caspase-3 (Cell Signaling Technology), or anti-phospho-Smad1/5/8 (Cell Signaling Technology). Membranes were stripped and reprobed with anti-Smad1 (Cell Signaling Technology), anti-β-actin (Sigma), or anti-GAPDH (Santa Cruz Biotechnology) antibodies.

RNA Isolation and Real Time PCR Analysis—Total RNA was isolated from kidneys or IMCD3 cells using the Pure Link™ RNA mini kit (Ambion) according to the manufacturer's instructions. For tissues, the QIAShredder (Qiagen) columns were used to filter the lysates, and the supernatants were collected to extract total RNA. First-strand cDNA synthesis was performed using the PrimeScript® RT reagent kit (TAKARA) and amplified using the ABI Prism 7900 Sequence Detection System (PE Biosystems).

Statistical Analysis—All data are represented as the mean ± S.D. of independent replicates ($n \geq 3$). Student's t test was applied for statistical analysis. A p value of ≤ 0.05 was considered statistically significant.

RESULTS

Dragon Increased Hypoxia-induced Cell Death in IMCD3 Kidney Tubular Epithelial Cells—To explore the role of Dragon in renal epithelial cell death/apoptosis, we first generated con-

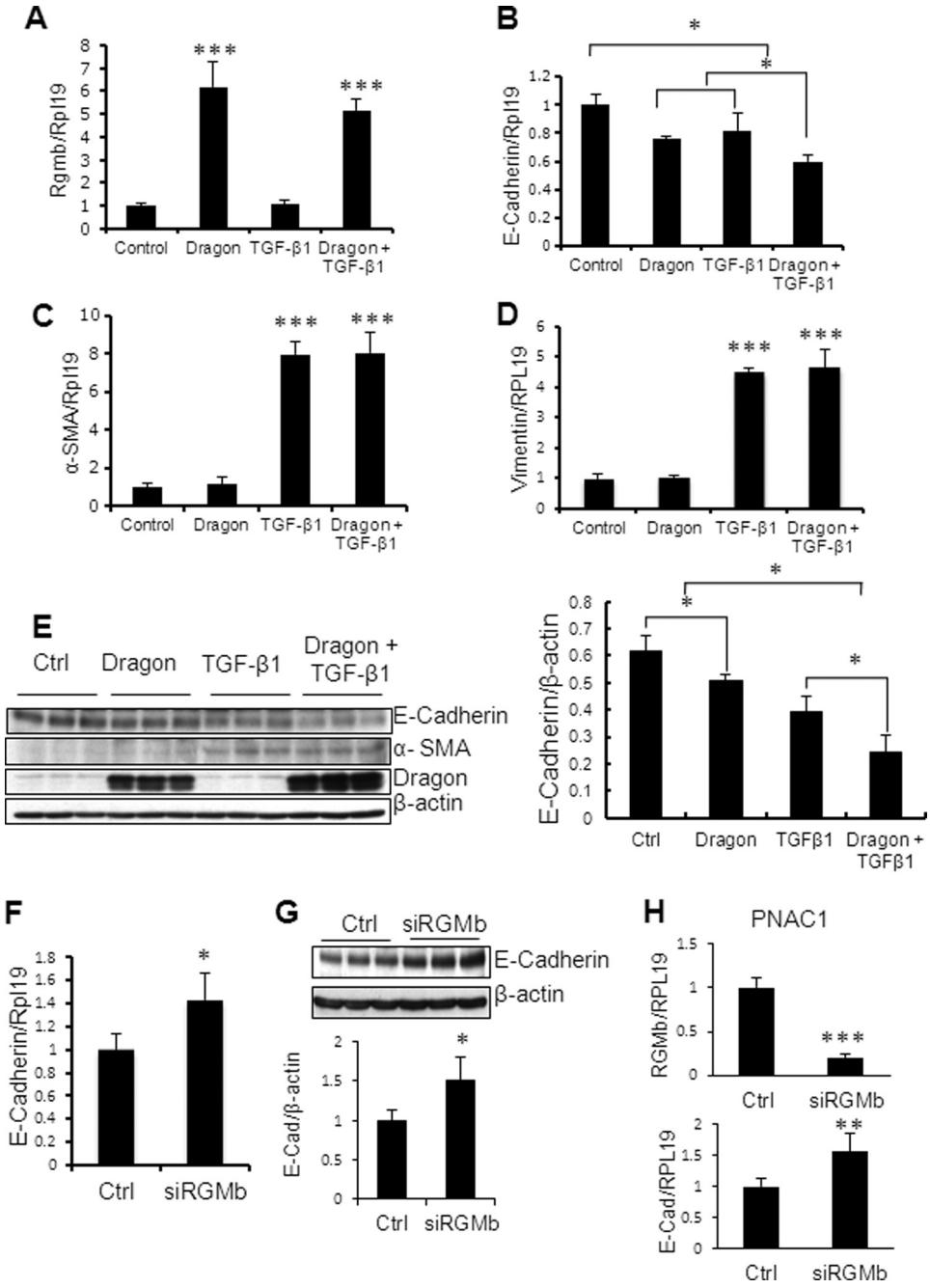

FIGURE 4. **Dragon (RGMb) inhibits E-cadherin expression but does not affect TGF-β1-induced EMT.** (*A–D*, effects of Dragon overexpression on expression of E-cadherin, α-SMA, and vimentin mRNAs in IMCD3 cells. Cells were transiently transfected with control plasmid or Dragon cDNA. 24 h after the transfection the cells were treated with or without TGF-β1 (5 ng/ml) for 48 h before the cells were collected for real time PCR analysis for Rgmb, E-cadherin, α-SMA, and vimentin mRNA levels. *E*, effects of Dragon overexpression on expression of E-cadherin and α-SMA proteins in IMCD3 cells. Cells were transiently transfected with control plasmid or Dragon cDNA. 24 h after the transfection the cells were treated with or without TGF-β1 (10 ng/ml) for 72 h before the cells were collected for Western blotting for Dragon (RGMb), E-cadherin, and α-SMA proteins (*left panel*, Western blots; *right panel*, densitometric analysis of E-cadherin relative to β-actin). *F* and *G*, inhibition of Dragon expression increased E-cadherin expression in IMCD3 cells. Cells were transfected with control siRNA or RGMb siRNA. 48 h after transfection, cells were harvested for real time PCR analysis for E-cadherin mRNA levels (*F*) or for Western blotting for E-cadherin protein levels (*G*, *top panel*, Western blots; *bottom panel*, densitometric analysis of the E-cadherin bands). *H*, inhibition of Dragon expression increased E-cadherin mRNA expression in PNAC1 cells. Cells were transfected with control siRNA or RGMb siRNA. 48 h after transfection, cells were harvested for real time PCR analysis for RGMb (*A*) and E-cadherin (*B*) mRNA levels. *, $p < 0.05$; **, $p < 0.01$; ***, $p < 0.001$.

trol IMCD3 clones Ctrl #2 and Ctrl#6 and stable Dragon-overexpressing clones Dra#4 and Dra#10. As shown in Fig. 1*A*, Dra#4 and Dra#10 expressed high levels of Dragon protein.

Oxidant stress is a major insult that causes tubular epithelial cell apoptosis during kidney injury. Indeed, H_2O_2 (500 μM) induced cell death in both Ctrl#2 and Dra#4 (Fig. 1*B*) 48 h after the treatment, but there was no difference in cell viability between the two cell lines. Similar results were obtained with Ctrl#6 and Dra#10 (data not shown).

We also examined the effects of Dragon on cisplatin-induced cell death (Fig. 1*C*). Cisplatin induced cell death in a dose-dependent manner in both Ctrl#2 and Dra#4. There was no dif-

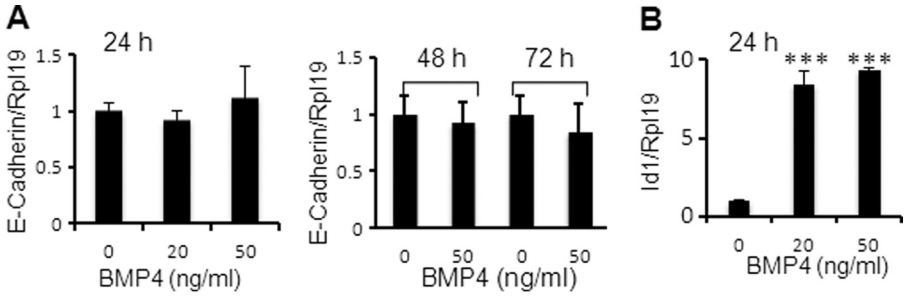

FIGURE 5. **BMP4 does not regulate E-cadherin expression in IMCD3 cells.** IMCD3 cells were treated with BMP4 for 24, 48, or 72 h before the cells were collected for real time PCR analysis for E-cadherin (*A*) or Id1 expression (*B*). Rpl19 is the internal control. ***, $p < 0.001$.

ference in the cell viability between the two clones in the presence of 6 μg/ml cisplatin. The viability was slightly decreased in Dra#4 compared with Ctrl#2 in the presence of 18 μg/ml cisplatin. These results suggest that Dragon does not play a major role in cell death induced by oxidant stress and cisplatin in tubular epithelial cells.

Previous studies revealed that hypoxia induces death of tubular epithelial cells via apoptosis (29, 30). Interestingly, the viability of cells cultured in 2% O_2 for 72 h normalized to the viability of cells cultured under normal conditions was significantly reduced in cells overexpressing Dragon (Dra#4 and Dra#10) compared with control cells (Ctrl#2 and Ctrl#6; Fig. 2*A*). Cleaved poly(ADP-ribose) polymerase (a marker for apoptosis) and cleaved caspase-3 (a marker for end-stage apoptosis) levels after 48 h of hypoxic culture were increased in Dra#10 (Fig. 2*B*) and Dra#4 (data not shown) compared with their respective controls.

To corroborate the results from Dragon stable cell lines, we performed transient transfection of Dragon cDNA. IMCD3 cells transfected with Dragon exhibited a decrease in cell viability (Fig. 2*C*) and an increase in cleaved caspase-3 (Fig. 2*D*) levels compared with control IMCD3 cells. Conversely, when Dragon expression was inhibited by 74.2% by siRNA targeting (Fig. 2*E*), hypoxia-induced cell viability was significantly increased (Fig. 2*F*). These results suggest that Dragon increases epithelial cell death/apoptosis induced by hypoxia.

Dragon Increased Hypoxia-induced Cell Death through Neogenin—Previous studies demonstrate that Dragon is a co-receptor that enhances BMP4 signaling (1, 6). To examine whether BMP signaling regulates hypoxia-induced cell death, we treated IMCD3 cells with increasing amounts of BMP4 and then cultured the cells in 2% O_2 for 72 h. As shown in Fig. 3*A*, BMP4 did not alter cell viability, suggesting that the BMP signaling does not play a role in hypoxia-induced cell death in IMCD3 cells.

To determine whether neogenin mediates Dragon action on cell death, we used neogenin siRNA to inhibit neogenin expression. Transfection of neogenin siRNA reduced neogenin mRNA expression by 59.4% (Fig. 3*B*, *left panel*) and increased cell viability (Fig. 3*B*, *right panel*) in IMCD3 cells cultured in hypoxia. Dragon overexpression inhibited cell viability, and inhibition of neogenin expression restored the cell viability in cells transfected with Dragon to the control levels (Fig. 3*C*). Interestingly, double inhibition of Dragon and neogenin expression further increased cell viability over inhibition of Dragon or neogenin alone (Fig. 3*D*). These results suggest that Dragon increases hypoxia-induced cell death through the neogenin receptor.

Dragon Inhibited E-cadherin Expression but Did Not Affect TGF-β1-induced α-SMA and Vimentin Expression in IMCD3 Cells—To examine whether Dragon antagonizes TGF-β1-induced EMT, we first established the time-course of 0.5, 1, 2, 4, 8, 24, 48, and 72 h for TGF-β1 treatment in IMCD3 cells. E-cadherin started to decrease at 24 h and further decreased at 48 and 72 h after TGF-β1 treatment (data not shown). α-SMA started to increase at 8 h and reached the peak at 48 h after TGF-β1 treatment (data not shown). Vimentin also started to increase at 8 h, and it kept increasing from 8 to 72 h after TGF-β1 treatment (data not shown). Based on the time courses, we chose TGF-β1 treatment for 48 h for further studies.

In the absence of TGF-β1, Dragon overexpression inhibited E-cadherin mRNA and protein expression (Fig. 4, *A*, *B*, and *E*). TGF-β1 treatment also inhibited E-cadherin mRNA and protein expression (Fig. 4, *B* and *E*), and Dragon overexpression further reduced E-cadherin expression at both mRNA (Fig. 4*B*) and protein (Fig. 4*E*) levels. Dragon overexpression had no effect on the basal and TGF-β1-induced α-SMA mRNA (Fig. 4*C*) or protein (Fig. 4*E*, *left panel*) and on the basal and TGF-β1-induced vimentin mRNA expression (Fig. 4*D*). These results suggest that Dragon does not regulate TGF-β1-induced EMT, although it inhibits E-cadherin expression.

To further study the role of Dragon in E-cadherin expression, we used Dragon siRNA to inhibit Dragon expression in IMCD3 cells. Inhibition of Dragon significantly increased E-cadherin mRNA (Fig. 4*F*) and protein expression (Fig. 4*G*) in IMCD3 cells. Interestingly, inhibition of Dragon expression also increased E-cadherin expression in PNAC1 human pancreatic epithelioid carcinoma cells (Fig. 4*H*).

Dragon Inhibited E-cadherin Expression through Neogenin—We first examined whether BMP4 signaling regulates E-cadherin expression. We treated IMCD3 cells with BMP4 for 24, 48, and 72 h. As shown in Fig. 5, BMP4 treatment did not alter E-cadherin, although it increased the expression of Id-1, a well known target gene of the BMP pathway, in IMCD3 cells. These results suggest that the BMP pathway is not involved in the regulation of E-cadherin by Dragon.

We then examined whether neogenin mediates Dragon's action on E-cadherin expression. Inhibition of neogenin significantly increased E-cadherin mRNA (Fig. 6*A*) and protein (Fig. 6*B*) expression in IMCD3 cells. Inhibition of neogenin expression also increased E-cadherin expression in PNAC1 cells (Fig. 6*C*). Dragon overexpression inhibited E-cadherin mRNA and

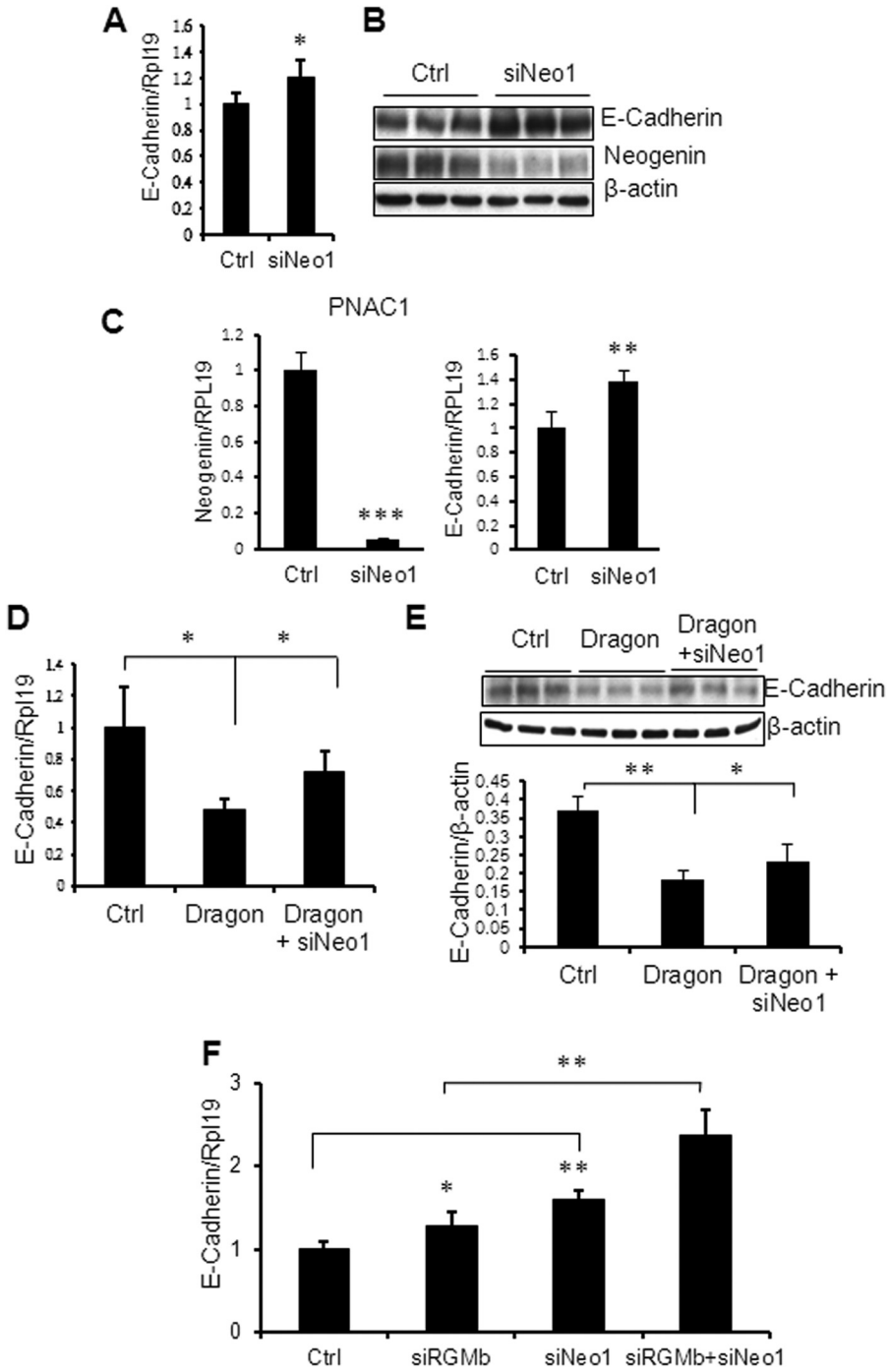

FIGURE 6. **Dragon (RGMb) inhibits E-cadherin expression through the neogenin receptor in IMCD3 cells.** *A*, effects of inhibition of neogenin expression on E-cadherin mRNA expression in IMCD3 cells. Cells were transfected with control siRNA or neogenin siRNA (*siNeo1*). 48 h after transfection cells were harvested for real time PCR analysis for neogenin and E-cadherin mRNA levels. *B*, effects of inhibition of neogenin expression on E-cadherin protein expression in IMCD3 cells. Cells were transfected with control siRNA or neogenin siRNA (*siNeo1*). 72 h after transfection, cells were harvested for Western blotting for E-cadherin and neogenin protein levels. *C*, effects of inhibition of neogenin expression on E-cadherin expression in PNAC1 cells. Cells were transfected with control siRNA or neogenin siRNA (*siNeo1*). 48 h after transfection cells were harvested for real time PCR analysis for neogenin and E-cadherin mRNA levels. *D* and *E*, inhibition of neogenin expression restored E-cadherin mRNA and protein expression suppressed by Dragon in IMCD3 cells. IMCD3 cells were transfected with Dragon cDNA or Dragon cDNA in combination of neogenin siRNA (*siNeo1*). 72 h after transfection cells were harvested for real time PCR analysis for E-cadherin mRNA levels (*D*) or for Western blotting for E-cadherin protein levels (*E*: *top panel*, Western blotting; *bottom panel*, densitometric analysis). *F*, double inhibition of Dragon (RGMb) and neogenin synergistically increased E-cadherin expression. IMCD3 cells were transfected with RGMb siRNA (*siRGMb*), neogenin siRNA (*siNeo1*), or both. 48 h after transfection cells were harvested for real time PCR analysis for E-cadherin mRNA levels. Rpl19 and β-actin are the internal controls for real time PCR and Western blotting respectively. *, $p < 0.05$; **, $p < 0.01$; ***, $p < 0.001$.

protein expression in IMCD3 cells, and inhibition of neogenin expression restored the E-cadherin mRNA (Fig. 6*D*) and protein (Fig. 6*E*) expression toward the control levels. Moreover, double inhibition of both Dragon and neogenin expression significantly increased E-cadherin expression compared with the inductions in E-cadherin levels by Dragon inhibition alone and

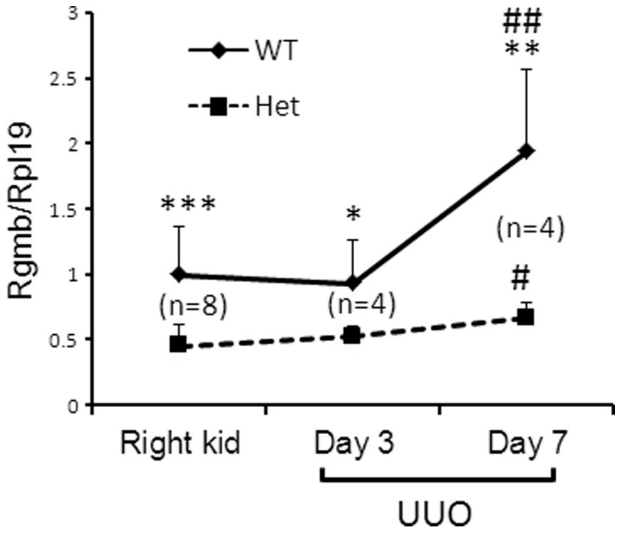

FIGURE 7. **Dragon expression in the kidney increases with UUO in WT and heterozygous Dragon knock-out (*Het*) mice.** Real time PCR analyses of Dragon in the left kidneys at days 3 and 7 after UUO from WT and Het mice at 3–4 months of age ($n = 4$). Right kidneys were subjected to sham operations and were used as control. Rpl19 is the internal control. *, **, and ***, WT *versus* Het; # and ##, left kidneys at 7 days post-UUO *versus* right kidneys. * or #, $p < 0.05$; ** or ##, $p < 0.01$; ***, $p < 0.001$.

neogenin inhibition alone (Fig. 6*F*). These results suggest that Dragon inhibits E-cadherin expression through the neogenin receptor.

Dragon$^{+/-}$ Mice Showed Decreased Tubular Epithelial Cell Apoptosis in Obstructed Kidneys—To support a biological role for Dragon in renal tubular epithelial cells *in vivo*, we studied heterozygous Dragon KO (Dragon$^{+/-}$) mice. Homozygous Dragon KO mice (Dragon$^{-/-}$) die within 2 weeks after birth (28), thus preventing us from using them to study the *in vivo* role of Dragon in kidney. Dragon$^{+/-}$ mice survive to adulthood and have no gross and histological abnormalities in the kidney. However, if there is any underlying defect in Dragon function in Dragon$^{+/-}$ mice, physiological stress may uncover the function.

We first examined whether Dragon expression changes with kidney injury in WT mice. Left kidneys were subjected to UUO, and the uninjured right kidneys were used as control. Dragon mRNA levels in the left kidneys at day 7 after UUO were significantly up-regulated compared with the left kidneys at day 3 after UUO and the right kidneys (Fig. 7, *WT*).

Dragon mRNA in the right kidneys of Dragon$^{+/-}$ mice was reduced by 55% compared with that in WT mice (Fig. 7). Dragon mRNA levels in the left kidneys at days 3 and 7 after UUO were reduced by 45 and 66%, respectively, in Dragon$^{+/-}$ mice compared with WT mice (Fig. 7).

We then performed TUNEL staining to quantitate apoptotic cells in WT and Dragon$^{+/-}$ kidneys after UUO (Fig. 8). UUO induced apoptosis in the tubules of the left kidneys 3 (Fig. 8, *A*, *C*, and *D*) and 7 days (Fig. 8, *B*, *C*, and *D*) after UUO in WT mice. UUO-induced apoptosis was dramatically suppressed in the left kidneys of Dragon$^{+/-}$ mice 3 and 7 days after UUO (Fig. 8, *A*–*D*). Cleaved caspase-3 in the left kidneys at day 7 after UUO was reduced in Dragon$^{+/-}$ mice compared with WT mice (Fig. 8*E*). These results suggest that Dragon promotes UUO-induced renal tubular epithelial cell apoptosis *in vivo*.

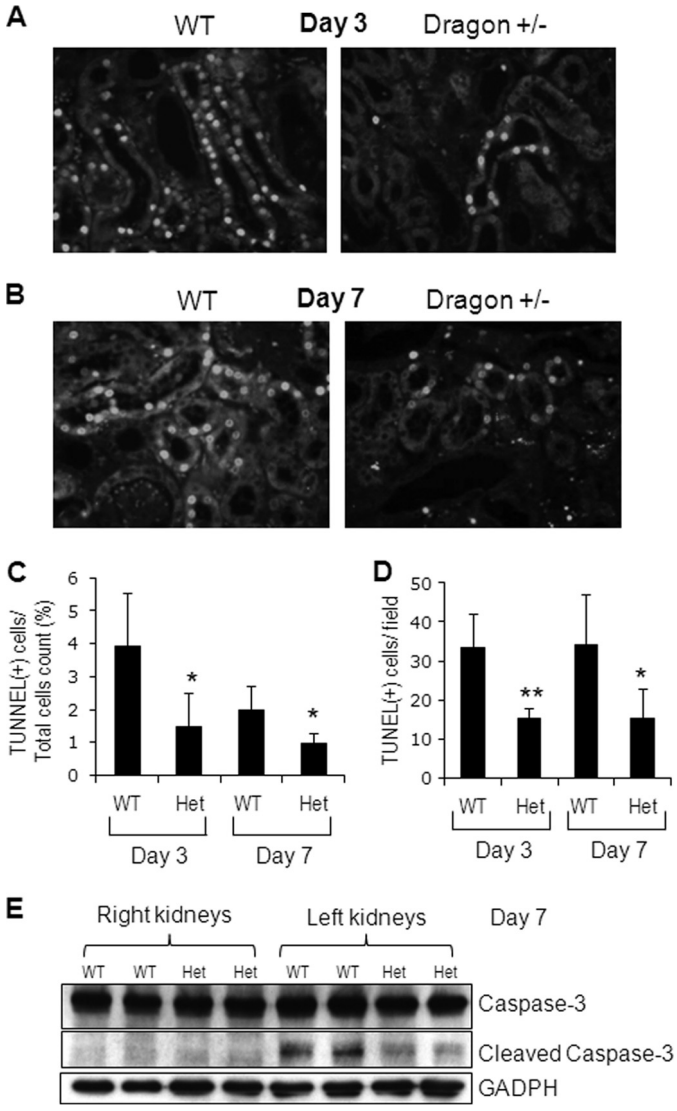

FIGURE 8. **Dragon$^{+/-}$ mice show decreased epithelial apoptosis in obstructed kidneys.** *A* and *B*, WT and Dragon$^{+/-}$ mice at 3–4 months of age were subjected to UUO on the left ureters. 3 and 7 days later the kidneys were collected for TUNEL assays to identify apoptotic cells in renal tubules. *C* and *D*, TUNEL-positive tubular epithelial cells were counted against the total number of cells (*C*) or in each field (*D*). Apoptotic-positive cells or total cells were counted in 10 random 400× fields. *E*, right kidneys (control) and left kidneys (obstructed) at 7 days post-UUO were subjected to Western blotting using caspase-3 antibody, which recognizes both full-length and cleaved caspase-3. *, $p < 0.05$; **, $p < 0.01$.

Dragon$^{+/-}$ Mice Showed Increased E-cadherin Expression in the Renal Tubular Cells of Kidneys after UUO—We compared the expression of E-cadherin, a marker for tubular epithelial integrity (31), in the kidneys at days 3 and 7 after UUO between WT and Dragon$^{+/-}$ mice. E-cadherin mRNA levels were decreased in kidneys at day 3 after UUO compared with the control right kidneys in WT mice, whereas they remained unchanged between the right and the obstructed kidneys in Dragon$^{+/-}$ mice (Fig. 9*A*, *Day 3*). Thus, E-cadherin mRNA levels in the kidneys at day 3 post-UUO were higher in Dragon$^{+/-}$ mice than in WT mice (Fig. 9*A*, *Day 3*). However, 7 days after UUO, E-cadherin mRNA expression was no longer different between the two genotypes and between control and obstructed kidneys (Fig. 9*A*, *Day 7*). Like E-cadherin mRNA,

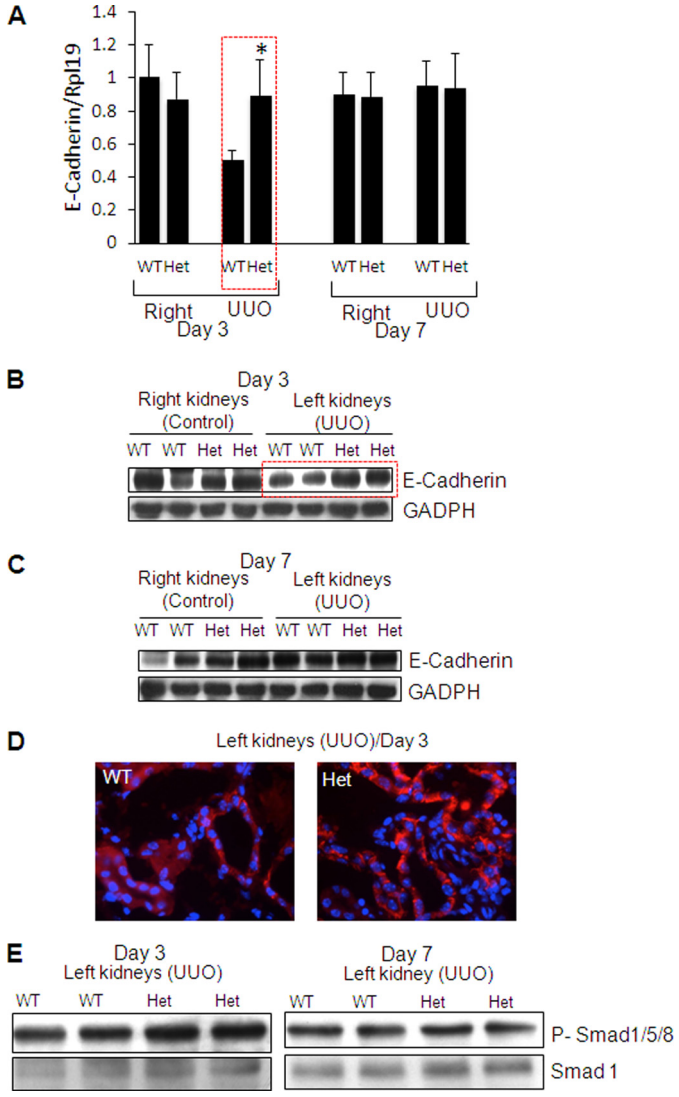

FIGURE 9. **Dragon$^{+/-}$ mice show increased E-cadherin expression in obstructed kidneys at day 3 post-UUO.** *A*, WT and Dragon$^{+/-}$ (*Het*) mice at 3–4 months of age were subjected to UUO on the left ureters. 3 and 7 days later, the kidneys were collected for real time PCR analysis for E-cadherin mRNA levels. All the values were normalized to the values in WT right kidneys at day 3 after UUO. *B* and *C*, right kidneys (control) and left kidneys (obstructed) were collected 3 (*B*) and 7 (*C*) days after UUO for Western blotting analysis for E-cadherin protein expression. GAPDH was used loading control. The *red rectangle* indicates reduced E-cadherin expression in WT compared with Het. *D*, immunofluorescence of E-cadherin (*red*) in obstructed (*left*) kidneys of WT and Dragon$^{+/-}$ (Het) at day 3 after UUO. DAPI (*blue*) was used for nuclear staining. *E*, obstructed (*left*) kidneys of WT and Het mice at days 3 and 7 after UUO were used for Western blotting for phospho-Smad1/5/8 and total Smad1. *, $p < 0.05$, Het *versus* WT in left kidneys 3 days after UUO.

E-cadherin protein expression was inhibited by UUO for 3 days in WT mice; thus, E-cadherin proteins levels were higher in Dragon$^{+/-}$ than in WT kidneys (Fig. 9*B*). In the kidneys at day 7 after UUO, E-cadherin proteins levels were similar between the two genotypes (Fig. 9*C*). As determined by immunofluorescence, E-cadherin was predominantly localized to the tubular epithelial cells in the kidneys at day 3 post-UUO, and the staining was stronger in Dragon$^{+/-}$ than in WT mice (Fig. 9*D*). Interestingly, Smad1/5/8 phosphorylation levels in UUO kidneys at day 3 or 7 after UUO were similar between WT and Dragon$^{+/-}$ mice (Fig. 9*E*). The results suggest that Dragon suppresses E-cadherin expression in renal tubular epithelial cells *in vivo*, and this activity may not be achieved via the BMP pathway.

UUO-induced Renal Fibrosis, and Inflammation Did Not Change between WT and Dragon$^{+/-}$ Mice—To examine whether Dragon plays a role in UUO-induced kidney fibrosis, we measured α-SMA, vimentin, and collagen I expression. α-SMA mRNA and protein levels were increased by UUO for 3 or 7 days in both WT and Dragon$^{+/-}$ kidneys, but no differences were found between the two genotypes (data not shown). Vimentin and collagen I mRNA levels were also up-regulated after UUO injury, and there was no difference between WT and Dragon$^{+/-}$ mice (data not shown). In addition, Masson's Trichrome staining did not detect any significant differences in fibrosis in obstructed kidneys between WT and Dragon$^{+/-}$ mice (Fig. 10*A*).

mRNA levels for inflammatory factors IL-6, TNF-α, MCP-1, and TGF-β1 were dramatically increased in the left kidneys at day 3 or 7 by UUO, but again, there was no difference between WT and Dragon$^{+/-}$ mice (data not shown). As determined by immunostaining for F4/80, there was macrophage infiltration in the kidneys subjected to UUO (data not shown). However, F4/80-positive cell numbers were not different between WT and Dragon$^{+/-}$ mice (data not shown). All these results suggest that Dragon may not play a role in the pathogenesis of fibrosis and inflammation induced by UUO.

Dragon$^{+/-}$ Mice Showed Ameliorated Tubular Injury after UUO—As shown by periodic acid-Schiff staining (Fig. 10*B*), the obstructed kidneys showed severe dilation/atrophy of renal tubules at day 7 after UUO in WT mice. Dragon$^{+/-}$ mice exhibited less severe morphological injury in the cortex, characterized by less tubular dilation and atrophy (Fig. 10*B*). Quantitative assessment of cortical tubular injury between WT and Dragon$^{+/-}$ mice is presented in Fig. 10*C*. WT and Dragon$^{+/-}$ showed similar structures in obstructed kidneys at 3 days after UUO. Together, our results suggest that Dragon may facilitate tubular injury, although it may not have a detectable role in renal fibrogenesis in obstructed kidneys.

DISCUSSION

Previous studies have shown that Dragon is expressed in many tissues and organs including the neural tissues and kidney (5, 6). However, the biological role of Dragon is largely unknown. Our previous study demonstrated that Dragon is localized in the tubular epithelial cells of mouse kidneys (6). In the present study we found that Dragon increased epithelial cell apoptosis induced by hypoxia in IMCD3 cells. In addition, we demonstrated that Dragon$^{+/-}$ mice had reduced renal epithelial cell apoptosis in obstructed kidneys compared with WT mice. Thus, for the first time to our knowledge, we provide evidence that Dragon promotes tubular epithelial cell apoptosis both *in vitro* and *in vivo*.

We recently identified Dragon as a BMP co-receptor that enhances BMP2 and BMP4 signaling in many cell types. Mounting evidence suggests that BMP signaling plays a protective role in renal injury in several models of chronic renal injury including obstruction, diabetes mellitus, and systemic lupus erythematosis (9–13). For example, exogenous BMP-7

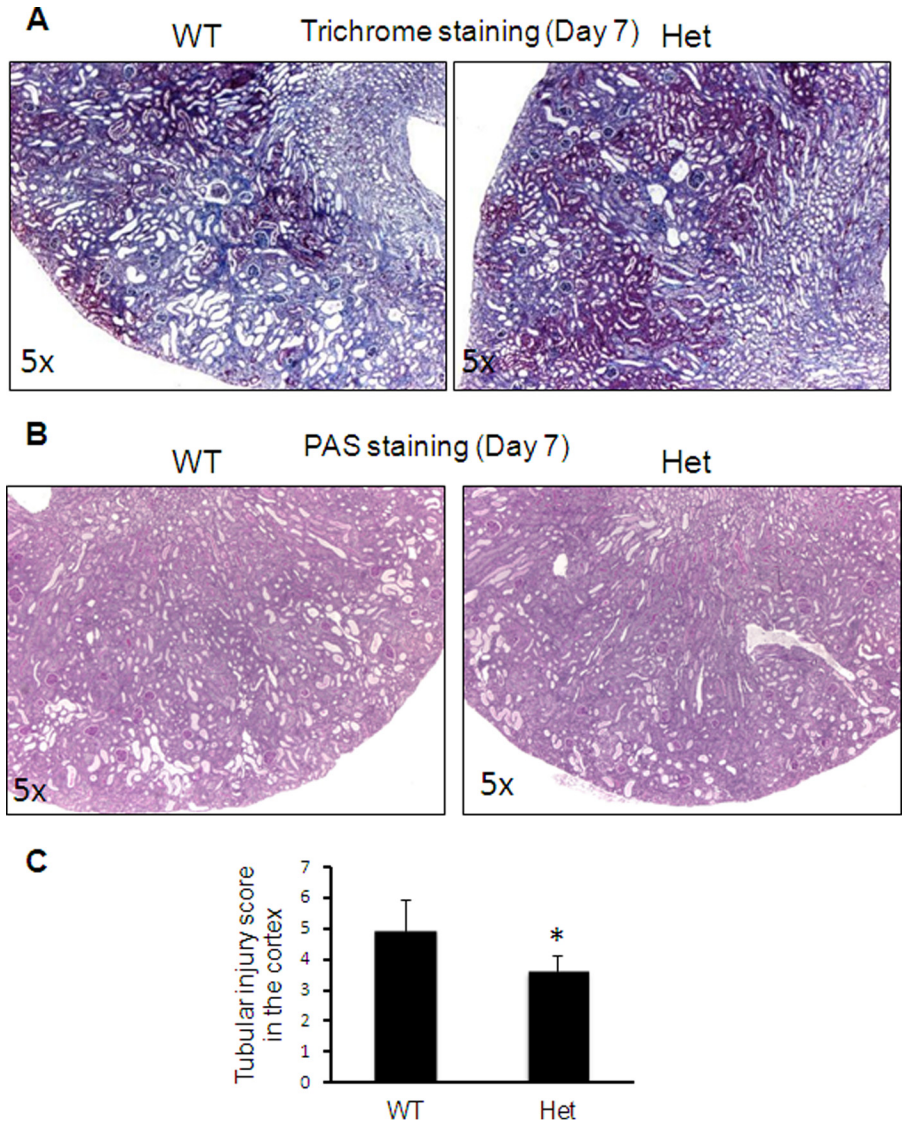

FIGURE 10. **Renal histology in Dragon$^{+/-}$ (*Het*) mice and WT mice after UUO injury.** Kidney sections obtained 7 days after UUO in WT and Het mice were subjected to Masson Trichrome staining (*A*) or periodic acid-Schiff staining (*B*). Pictures display representative areas of kidneys from WT and Het mice. Quantitative assessment of tubular injury in the cortex on periodic acid-Schiff -stained sections is presented (*C*).

reversed EMT and improved functional and pathologic markers of renal injury (9), whereas USAG-1, a BMP7 antagonist, accelerates renal injury (10). Therefore, one would expect that Dragon antagonizes TGF-β1-induced EMT *in vitro* and protects tubular epithelium from injury *in vivo*. In contrast, our present study demonstrated that Dragon did not have any effect on EMT induced by TGF-β1 in IMCD3 cells. Reduction in Dragon expression by 50% in Dragon$^{+/-}$ mice suppressed tubular apoptosis, sustained E-cadherin expression, and ameliorated tubular injury in obstructed kidneys. These results suggest that Dragon may play a detrimental role in renal tubules in UUO-induced kidney injury. Therefore, the BMP signaling function of Dragon did not have a significant protective role in tubular injury in the kidney.

After urinary tract obstruction, renal tubules undergo a rapid loss of tubular epithelial cell integrity and cell polarity. Normal cell-cell and cell-matrix interactions are disrupted during injury. All these changes result in tubular cell apoptosis and necrosis, ultimately leading to tubular atrophy. Compared with WT mice, Dragon$^{+/-}$ mice showed reduced tubular epithelial apoptosis after UUO. Heterozygous knock-out of Dragon prevented E-cadherin loss in the kidneys at day 3 after UUO. Because E-cadherin is critically involved in formation of epithelial cell-cell junctions and generation of a polarized epithelial phenotype (31), it is tempting to speculate that the maintenance of E-cadherin expression and epithelial integrity may at least partially contribute to the reduced epithelial apoptosis observed in Dragon$^{+/-}$ mice.

E-cadherin expression in the contralateral kidneys was not different between Dragon$^{+/-}$ and WT mice. In addition, E-cadherin expression in the injured kidneys of WT mice recovered despite the induction of Dragon expression at day 7 after UUO. These results suggest that some unknown permissive conditions may be required to allow Dragon to exert its inhibitory action on E-cadherin. These conditions may exist in the injured kidneys at day 3 after UUO but not in the contralateral kidneys or the injured kidneys at day 7 after UUO.

The RGMa-neogenin interaction plays a role in regulating neurite outgrowth and neuronal survival in the CNS (32, 33), in inducing cell death during *Xenopus* development (34) and in colorectal cancer cells (35), as well as in controlling inflammatory response in tissue injury (36, 37). In the present study we found that Dragon increased cell apoptosis and inhibited E-cadherin expression through the neogenin receptor but not the BMP pathway in IMCD3 cells. Whether this mechanism is responsible for the changes in tubular cell apoptosis and E-cadherin expression seen in Dragon$^{+/-}$ mice remains to be established.

We examined whether Dragon regulates the transcription factors that are critically involved in E-cadherin expression. Neither overexpression of Dragon nor inhibition of Dragon expression altered Snail, Twist, Zeb1, and Sip1 mRNA expression (data not shown). Thus, the mechanisms responsible for the action of Dragon/neogenin on E-cadherin remain to be defined.

Recent studies showed that during UUO injury, the tubular epithelial cells lose E-cadherin expression but the cells do not gain mesenchymal markers including vimentin and α-SMA (25–27). This indicates that transformation into myofibroblasts is not the epithelial cell fate in obstructive nephropathy. Interestingly, our results showed that overexpression of Dragon inhibited E-cadherin expression but failed to alter vimentin and α-SMA expression in IMCD3 cells. All these data support the notion that disruption of epithelial integrity does not necessarily result in EMT.

Apoptosis plays an important role in inflammation and subsequent renal injury (19, 22). Apoptotic tubular epithelial cells secrete many signaling molecules such as proinflammatory chemokines and cytokines. These molecules induce the infiltration of circulating leukocytes including monocytes and neutrophils, which further enhance the ongoing inflammation (38). In the present study we did not see any differences between Dragon$^{+/-}$ and WT mice in expression of IL-6, TNF-α, MCP-1, and TGF-β1 and in macrophage infiltration in obstructed kidneys despite the reduced tubular apoptosis in Dragon$^{+/-}$ mice. The failure of Dragon$^{+/-}$ mice to exhibit any changes in UUO-induced inflammation could be multifactorial. One possibility is that UUO induces very severe injury that may have overwhelmed the small changes in inflammation induced by apoptosis.

In the obstructive kidney, the major stresses include mechanical stretching, oxidant stress, and hypoxia. In IMCD3 cells, Dragon increased hypoxia-induced cell death but had no effect on cell death caused by oxidant stress. Whether Dragon plays a role in epithelial cell death induced by mechanical stretching is unknown.

Homozygous Dragon knock-out mice die between 2 and 3 weeks after birth. Heterozygous Dragon knock-out mice survive to adulthood, but they do not have detectable histological and functional kidney abnormalities. Therefore, the physiological role of Dragon in normal kidney function will remain unknown until tubular cell-specific Dragon KO mice are available.

In summary, we have demonstrated that Dragon promoted hypoxia-induced cell death/apoptosis and inhibited E-cadherin expression through neogenin in IMCD3 cells. Dragon$^{+/-}$ mice had decreased epithelial apoptosis, increased epithelial E-cadherin expression, and less injured tubules in obstructed kidneys compared with WT mice. Our results suggest that Dragon may play a detrimental role in kidney tubular injury by impairing tubular epithelial integrity and inducing epithelial cell apoptosis in obstructive nephropathy.

Acknowledgment—We thank Dr. Bo Feng for sharing the E-cadherin antibodies.

REFERENCES

1. Samad, T. A., Rebbapragada, A., Bell, E., Zhang, Y., Sidis, Y., Jeong, S. J., Campagna, J. A., Perusini, S., Fabrizio, D. A., Schneyer, A. L., Lin, H. Y., Brivanlou, A. H., Attisano, L., and Woolf, C. J. (2005) DRAGON, a bone morphogenetic protein co-receptor. *J. Biol. Chem.* **280,** 14122–14129
2. Babitt, J. L., Zhang, Y., Samad, T. A., Xia, Y., Tang, J., Campagna, J. A., Schneyer, A. L., Woolf, C. J., and Lin, H. Y. (2005) Repulsive guidance molecule (RGMa), a DRAGON homologue, is a bone morphogenetic protein co-receptor. *J. Biol. Chem.* **280,** 29820–29827
3. Babitt, J. L., Huang, F. W., Wrighting, D. M., Xia, Y., Sidis, Y., Samad, T. A., Campagna, J. A., Chung, R. T., Schneyer, A. L., Woolf, C. J., Andrews, N. C., and Lin, H. Y. (2006) Bone morphogenetic protein signaling by hemojuvelin regulates hepcidin expression. *Nat. Genet.* **38,** 531–539
4. Xia, Y., Yu, P. B., Sidis, Y., Beppu, H., Bloch, K. D., Schneyer, A. L., and Lin, H. Y. (2007) Repulsive guidance molecule (RGMa) alters utilization of bone morphogenetic protein (BMP) type II receptors by BMP2 and BMP4. *J. Biol. Chem.* **282,** 18129–18140
5. Xia, Y., Babitt, J. L., Sidis, Y., Chung, R. T., and Lin, H. Y. (2008) Hemojuvelin regulates hepcidin expression via a selective subset of BMP ligands and receptors independently of neogenin. *Blood* **111,** 5195–5204
6. Xia, Y., Babitt, J. L., Bouley, R., Zhang, Y., Da Silva, N., Chen, S., Zhuang, Z., Samad, T. A., Brenner, G. J., Anderson, J. L., Hong, C. C., Schneyer, A. L., Brown, D., and Lin, H. Y. (2010) Dragon enhances BMP signaling and increases transepithelial resistance in kidney epithelial cells. *J. Am. Soc. Nephrol.* **21,** 666–677
7. Cain, J. E., Hartwig, S., Bertram, J. F., and Rosenblum, N. D. (2008) Bone morphogenetic protein signaling in the developing kidney. Present and future. *Differentiation* **76,** 831–842
8. Gould, S. E., Day, M., Jones, S. S., and Dorai, H. (2002) BMP-7 regulates chemokine, cytokine, and hemodynamic gene expression in proximal tubule cells. *Kidney Int.* **61,** 51–60
9. Zeisberg, M., Hanai, J., Sugimoto, H., Mammoto, T., Charytan, D., Strutz, F., and Kalluri, R. (2003) BMP-7 counteracts TGF-β1-induced epithelial-to-mesenchymal transition and reverses chronic renal injury. *Nat. Med.* **9,** 964–968
10. Yanagita, M., Okuda, T., Endo, S., Tanaka, M., Takahashi, K., Sugiyama, F., Kunita, S., Takahashi, S., Fukatsu, A., Yanagisawa, M., Kita, T., and Sakurai, T. (2006) Uterine sensitization-associated gene-1 (USAG-1), a novel BMP antagonist expressed in the kidney, accelerates tubular injury. *J. Clin. Invest.* **116,** 70–79
11. Yang, Y. L., Liu, Y. S., Chuang, L. Y., Guh, J. Y., Lee, T. C., Liao, T. N., Hung, M. Y., and Chiang, T. A. (2009) Bone morphogenetic protein-2 antagonizes renal interstitial fibrosis by promoting catabolism of type I transforming growth factor-β receptors. *Endocrinology* **150,** 727–740
12. Dendooven, A., van Oostrom, O., van der Giezen, D. M., Leeuwis, J. W., Snijckers, C., Joles, J. A., Robertson, E. J., Verhaar, M. C., Nguyen, T. Q., and Goldschmeding, R. (2011) Loss of endogenous bone morphogenetic protein-6 aggravates renal fibrosis. *Am. J. Pathol.* **178,** 1069–1079
13. Meng, X. M., Chung, A. C., and Lan, H. Y. (2013) Role of the TGF-β/BMP-7/Smad pathways in renal diseases. *Clin. Sci.* **124,** 243–254
14. Conrad, S., Stimpfle, F., Montazeri, S., Oldekamp, J., Seid, K., Alvarez-Bolado, G., and Skutella, T. (2010) RGMb controls aggregation and migration of neogenin-positive cells *in vitro* and *in vivo*. *Mol. Cell. Neurosci.* **43,** 222–231

15. Bell, C. H., Healey, E., van Erp, S., Bishop, B., Tang, C., Gilbert, R. J., Aricescu, A. R., Pasterkamp, R. J., and Siebold, C. (2013) Structure of the repulsive guidance molecule (RGM)-neogenin signaling hub. *Science* **341,** 77–80
16. Wang, W., and Ramesh, G. (2009) Segment-specific expression of Netrin-1 receptors in normal and ischemic mouse kidney. *Am. J. Nephrol.* **30,** 186–193
17. Bascands, J. L., and Schanstra, J. P. (2005) Obstructive nephropathy. Insights from genetically engineered animals. *Kidney Int.* **68,** 925–937
18. Liu, Y. (2006) Renal fibrosis. New insights into the pathogenesis and therapeutics. *Kidney Int.* **69,** 213–217
19. Docherty, N. G., O'Sullivan, O. E., Healy, D. A., Fitzpatrick, J. M., and Watson, R. W. (2006) Evidence that inhibition of tubular cell apoptosis protects against renal damage and development of fibrosis following ureteric obstruction. *Am. J. Physiol. Renal Physiol.* **290,** F4–F13
20. Zeisberg, M., and Neilson, E. G. (2010) Mechanisms of tubulointerstitial fibrosis. *J. Am. Soc. Nephrol.* **21,** 1819–1834
21. Truong, L. D., Petrusevska, G., Yang, G., Gurpinar, T., Shappell, S., Lechago, J., Rouse, D., and Suki, W. N. (1996) Cell apoptosis and proliferation in experimental chronic obstructive uropathy. *Kidney Int.* **50,** 200–207
22. Daemen, M. A., van 't Veer, C., Denecker, G., Heemskerk, V. H., Wolfs, T. G., Clauss, M., Vandenabeele, P., and Buurman, W. A. (1999) Inhibition of apoptosis induced by ischemia-reperfusion prevents inflammation. *J. Clin. Invest.* **104,** 541–549
23. Liu, Y. (2010) New insights into epithelial-mesenchymal transition in kidney fibrosis. *J. Am. Soc. Nephrol.* **21,** 212–222
24. Zeisberg, M., and Duffield, J. S. (2010) Resolved. EMT produces fibroblasts in the kidney. *J. Am. Soc. Nephrol.* **21,** 1247–1253
25. Humphreys, B. D., Valerius, M. T., Kobayashi, A., Mugford, J. W., Soeung, S., Duffield, J. S., McMahon, A. P., and Bonventre, J. V. (2008) Intrinsic epithelial cells repair the kidney after injury. *Cell Stem Cell* **2,** 284–291
26. Humphreys, B. D., Lin, S. L., Kobayashi, A., Hudson, T. E., Nowlin, B. T., Bonventre, J. V., Valerius, M. T., McMahon, A. P., and Duffield, J. S. (2010) Fate tracing reveals the pericyte and not epithelial origin of myofibroblasts in kidney fibrosis. *Am. J. Pathol.* **176,** 85–97
27. Li, L., Zepeda-Orozco, D., Black, R., and Lin, F. (2010) Autophagy is a component of epithelial cell fate in obstructive uropathy. *Am. J. Pathol.* **176,** 1767–1778
28. Xia, Y., Cortez-Retamozo, V., Niederkofler, V., Salie, R., Chen, S., Samad, T. A., Hong, C. C., Arber, S., Vyas, J. M., Weissleder, R., Pittet, M. J., and Lin, H. Y. (2011) Dragon (repulsive guidance molecule b) inhibits IL-6 expression in macrophages. *J. Immunol.* **186,** 1369–1376
29. Khan, S., Cleveland, R. P., Koch, C. J., and Schelling, J. R. (1999) Hypoxia induces renal tubular epithelial cell apoptosis in chronic renal disease. *Lab. Invest.* **79,** 1089–1099
30. Hotter, G., Palacios, L., and Sola, A. (2004) Low O_2 and high CO_2 in LLC-PK1 cells culture mimics renal ischemia-induced apoptosis. *Lab. Invest.* **84,** 213–220
31. Yang, J., and Liu, Y. (2001) Dissection of key events in tubular epithelial to myofibroblast transition and its implications in renal interstitial fibrosis. *Am. J. Pathol.* **159,** 1465–1475
32. Rajagopalan, S., Deitinghoff, L., Davis, D., Conrad, S., Skutella, T., Chedotal, A., Mueller, B. K., and Strittmatter, S. M. (2004) Neogenin mediates the action of repulsive guidance molecule. *Nat. Cell Biol.* **6,** 756–762
33. Matsunaga, E., Tauszig-Delamasure, S., Monnier, P. P., Mueller, B. K., Strittmatter, S. M., Mehlen, P., and Chédotal, A. (2004) RGM and its receptor neogenin regulate neuronal survival. *Nat. Cell Biol.* **6,** 749–755
34. Shin, G. J., and Wilson, N. H. (2008) Overexpression of repulsive guidance molecule (RGM) a induces cell death through Neogenin in early vertebrate development. *J. Mol. Histol.* **39,** 105–113
35. Li, V. S., Yuen, S. T., Chan, T. L., Yan, H. H., Law, W. L., Yeung, B. H., Chan, A. S., Tsui, W. Y., So, S., Chen, X., and Leung S. Y. (2009) Frequent inactivation of axon guidance molecule RGMA in human colon cancer through genetic and epigenetic mechanisms. *Gastroenterology* **137,** 176–187
36. Mirakaj, V., Brown, S., Laucher, S., Steinl, C., Klein, G., Köhler, D., Skutella, T., Meisel, C., Brommer, B., Rosenberger, P., and Schwab, J. M. (2011) Repulsive guidance molecule-A (RGM-A) inhibits leukocyte migration and mitigates inflammation. *Proc. Natl. Acad. Sci. U.S.A.* **108,** 6555–6560
37. Muramatsu, R., Kubo, T., Mori, M., Nakamura, Y., Fujita, Y., Akutsu, T., Okuno, T., Taniguchi, J., Kumanogoh, A., Yoshida, M., Mochizuki, H., Kuwabara, S., and Yamashita, T. (2011) RGMa modulates T cell responses and is involved in autoimmune encephalomyelitis. *Nat. Med.* **17,** 488–494
38. Chung, A. C., and Lan, H. Y. (2011) Chemokines in renal injury. *J. Am. Soc. Nephrol.* **22,** 802–809